communications biology

Article

https://doi.org/10.1038/s42003-024-07229-8

Angiotensin-II drives changes in microglia–vascular interactions in rats with heart failure

Ferdinand Althammer[1,2], Ranjan K. Roy[1,3], Matthew K. Kirchner[1,3], Yuval Podpecan[2], Jemima Helen[2], Shaina McGrath[1,3], Elba Campos Lira[1,3] & Javier E. Stern[1,3]

Activation of microglia, the resident immune cells of the central nervous system, leading to the subsequent release of pro-inflammatory cytokines, has been linked to cardiac remodeling, autonomic disbalance, and cognitive deficits in heart failure (HF). While previous studies emphasized the role of hippocampal Angiotensin II (AngII) signaling in HF-induced microglial activation, unanswered mechanistic questions persist. Evidence suggests significant interactions between microglia and local microvasculature, potentially affecting blood–brain barrier integrity and cerebral blood flow regulation. Still, whether the microglial-vascular interface is affected in the brain during HF remains unknown. Using a well-established ischemic HF rat model, we demonstrate the increased abundance of vessel-associated microglia (VAM) in HF rat hippocampi, along with an increased expression of AngII AT1a receptors. Acute AngII administration to sham rats induced microglia recruitment to brain capillaries, along with increased expression of TNFα. Conversely, administering an AT1aR blocker to HF rats prevented the recruitment of microglia to blood vessels, normalizing their levels to those in healthy rats. These results highlight the critical importance of a rather understudied phenomenon (i.e., microglia-vascular interactions in the brain) in the context of the pathophysiology of a highly prevalent cardiovascular disease, and unveil novel potential therapeutic avenues aimed at mitigating neuroinflammation in cardiovascular diseases.

Heart failure (HF) is a complex clinical syndrome characterized by the inability of the heart to adequately pump blood and meet the body's metabolic demands[1]. It represents a significant public health concern worldwide due to its high prevalence, morbidity, mortality, and associated healthcare costs[1,2]. The burden of HF on society is substantial. According to the World Health Organization (WHO), an estimated 65 million people are affected by HF globally, and its prevalence is projected to increase due to aging populations and the rising prevalence of risk factors like obesity and diabetes[3,4]. Despite the clinical and economic impact of HF on society[2,3,5], precise mechanisms explaining the manifold peripheral, central, and systemic effects of this disease, as well as novel (sub-)cellular therapeutic targets are missing.

Research has increasingly highlighted the association between HF and cognitive deficits[6–9], with a spotlight on the hippocampus[6,10–13], a key player in memory and cognitive functions[14]. Studies have demonstrated that HF patients often exhibit structural and functional alterations in the hippocampus[6,12], contributing to cognitive impairment. The hippocampus is particularly vulnerable due to its sensitivity to changes in cerebral blood flow[15,16] and its susceptibility to the effects of neuroinflammation[17,18]. Emerging evidence suggests that neuroinflammation and microglial activation play a significant role in the progression of various cardiovascular diseases, including HF[19–24]. Microglia, the resident immune cells of the CNS, are known to become activated in response to injury, infection, or inflammation[25–27]. Importantly, their activation and the consequent release of pro-inflammatory cytokines have been shown to contribute to the progression of HF by affecting autonomic control, cardiac remodeling, and neuronal dysfunction[19,23,24]. The early stage of HF involves a myriad of different signaling cascades. One of the most important and best-studied signals overactivated during HF is the Angiotensin II (AngII)-AT1a receptor (AT1aR) cascade[28,29] including excessive AngII production and elevated circulating AngII levels[29–33].

Notably, a growing body of evidence supports the role of microglial AngII signaling in cognitive deficits associated with HF[19,34–36]. For example, activation of microglia by elevated levels of AngII induced

[1]Center for Neuroinflammation and Cardiometabolic Diseases, Georgia State University, Atlanta, GA, USA. [2]Institute of Human Genetics, Heidelberg University Hospital, Heidelberg, Germany. [3]Neuroscience Institute, Georgia State University, Atlanta, GA, USA. e-mail: jstern@gsu.edu

neuroinflammation in the hippocampus of HF rats, disrupting synaptic plasticity and impairing memory consolidation[10,19]. Moreover, we recently demonstrated that microglial AngII-AT1aR signaling precedes cytokine production in the hippocampus of HF rats, and that administration of the AT1R antagonist losartan improved various cellular, molecular, and behavioral endpoints in HF rats[19]. This interaction between AngII-AT1aR signaling, neuroinflammation, and cardiac dysfunction underscores the intricate link between the cardiovascular and central nervous systems in HF.

Microglia are not only involved in neuroinflammation but also play a crucial role in interacting with the local microvasculature. For example, microglia play a critical role in maintaining the integrity of the blood–brain barrier (BBB)[25,37–41]. Moreover, a growing body of evidence supports a direct role of microglia in regulating brain blood flow[42,43]. Importantly, a subset of microglia has been shown to have direct anatomical interactions with the local microvasculature, particularly brain capillaries. These include microglia with prominent somatic contact with blood capillaries, named by several groups as juxtavascular microglia[44,45], as well as microglial cells whose dynamic processes, but not their soma, are in contact with brain capillaries[46] (herein defined as vessel interacting microglia (VIMs). Together, these microglial cell types displaying intimate interaction with the local microvasculature have been defined as vessel-associated microglia (VAMs)[37,43]. In a recent study, Bisht and colleagues used in vivo 2-photon imaging to monitor microglial movements in the mouse cortex and found that microglia-vessel interactions are highly dynamic[43]. Moreover, Haruwaka and colleagues showed that during systemic inflammation, microglia migrate toward blood vessels and promote BBB stability through Claudin-5[37]. However, upon sustained inflammation, microglia begin to phagocytose astrocytic AQP4-positive endfeet in a CD68-dependent manner, thereby compromising BBB integrity[37]. Thus, these studies support the notion that microglia-vascular interactions are highly dynamic, both under physiological and pathological conditions. Still, whether the microglial-vascular interface in the hippocampus is affected in HF, and whether the AngII-AT1aR signaling cascade is a major contributing factor, remains completely unknown.

To address this major gap in our knowledge, in the current study we used a well-established rat model of ischemic HF and employed a multidisciplinary approach including immunohistochemistry, RNAScope hybridization, three-dimensional microglia/vascular reconstruction, in vivo intracarotid infusion of vessel markers and fluorescently-labeled AngII, and administration of the AT1R antagonist losartan. We specifically tested the hypothesis that the AngII-AT1aR signaling cascade contributes to dysregulation of the microglial-vascular interface in the hippocampus of rats with HF.

Results

Increased number of vessel-associated microglia (VAM) in HF rats

To explore the role of microglia-vessel interactions and to determine whether these interactions were altered in HF (see Table 1), we first stained brain sections containing the dorsal hippocampus (DH) of sham and HF rats with antibodies against the microglial marker IBA1 and the indirect vascular marker aquaporin-4 (AQP4[37,47,48]), to investigate potential differences in the number of parenchymal vs vessel-associated microglia (VAM) between the two groups (Fig. 1a, b). We found that AQP4 immunoreactive levels and distribution were comparable between sham and HF rats (Fig. S1a–c) However, we observed a significant increase in the proportion of VAM in HF rats (2.1-fold, Fig. 1c), which was accompanied by a reduction of parenchymal microglia. Thus, we analyzed the morphological properties of microglia that were either in close proximity of, or associated with, blood vessels in detail using Imaris algorithms (see "Methods"). We observed considerable variation among cells reflected by alterations in the overall shape and density of microglia-vessel interactions. Based on these quantitative properties and previously used classifications[43,46,49], we further classified vessel-associated microglia (VAM) into two subgroups (Fig. 1d): vessel-interacting microglia (VIM, i.e., microglia whose processes are directly touching brain capillaries[46] or juxtavascular (i.e., microglia with clear somatic vessel contact[37,43,45]) (see respective samples in Fig. 1d). Intriguingly, we found that the relative abundance of each individual VAM subtype was essentially reversed in HF rats. While VIM accounted for the majority of VAM in sham rats, juxtavascular microglia were the majority in HF rats (chi-square test, $p < 0.0001$, Fig. 1e).

Table 1 | Echocardiographic assessment of sham and HF rats used in this study

	Sham	HF	*p* value
Heart rate, (BPM)	297.53 ± 31.19	270.88 ± 24.44	n.s.
Stroke volume, (uL)	239.28 ± 34.89	126.03 ± 15.74	****
Ejection fraction, (%)	82.27 ± 3.2	25.22 ± 6.29	****
Fractional shortening, (%)	50.68 ± 3.92	14.36 ± 1.28	****
Cardiac output, (mL/min)	70.85 ± 10.82	34.23 ± 5.73	****
LV mass, (mg)	1846.48 ± 105.62	966.5 ± 113.42	****
Lvaw, d, (mm)	3.04 ± 0.54	1.46 ± 0.29	****
Lvaw, s, (mm)	3.67 ± 0.40	15.61 ± 56.36	****
Lvid, d, (mm)	6.9 ± 0.57	12.3 ± 1.37	****
Lvid, s, (mm)	4.43 ± 0.54	8.23 ± 0.69	****
Lvpw, d, (mm)	3.58 ± 0.47	1.55 ± 0.35	****
Lvpw, s, (mm)	3.68 ± 0.26	1.93 ± 0.26	****

****$p < 0.0001$.

Because AQP4 is a marker of astrocytic endfeet and only indirectly labels blood vessels, we performed a series of experiments involving co-staining with the endothelial maker CD31 (PECAM-1). We observed near-complete overlap between AQP4 and CD31 (>94%, Fig. S1d–f), and the average distance of reconstructed microglia from CD31 or AQP4 surfaces was virtually identical (Fig. S1h). In addition, and similarly to what we observed with AQP4, we replicated the finding of a significant increase in the proportion of VAM in HF rats using CD31 as a vascular marker (Fig. S1g).

Given that we previously reported morphological changes of hippocampal microglia in HF rats[19], we were curious whether juxtavascular microglia display similar alterations. However, while juxtavascular microglia were significantly less complex than parenchymal microglia, we found that juxtavascular microglia were morphologically not distinct between sham and HF rats (Fig. S2a).

Microglial AT1aRs overexpression and leaked AngII levels in HF rats

Circulating AngII levels dramatically increase in HF[1,30]. Moreover, we recently showed that AngII can gain access to the hippocampal parenchyma in HF rats[19], which is then taken up by microglia that overexpress AngII AT1a receptors (AT1aRs), initiating a neuroinflammatory cascade leading to neuronal deterioration and apoptosis in HF rats[19]. However, it remained unclear whether AT1R overexpression and leaked AngII uptake during HF occurs in parenchymal microglia or VAM. To this end, we first combined immunohistochemical staining to label microglia and vessels with RNA-Scope for AT1aR mRNA (Fig. 2a, b). Intriguingly, our results show that virtually all VAM were AT1aR mRNA-positive, both in sham and HF rats (Fig. 2c), a proportion that was significantly higher than that observed in parenchymal microglia ($p < 0.0001$, F (3, 21) = 230.8, two-way ANOVA). Conversely, we found that an increased proportion of microglia expressing AT1aR mRNA was observed only in parenchymal microglial cells ($p < 0.0001$, F (3, 21) = 230.8, two-way ANOVA). Intriguingly, albeit the proportion of AT1aR-positive VAM did not differ between sham and HF rats, we observed a significant increase of AT1aR mRNA puncta in this population in HF rats (Fig. 2d). Collectively, these results support an increased AT1aR expression in both populations on microglia in HF rats.

To further determine whether the leaked AngII during HF involves binds to both parenchymal microglia and/or VAM, we performed a new set

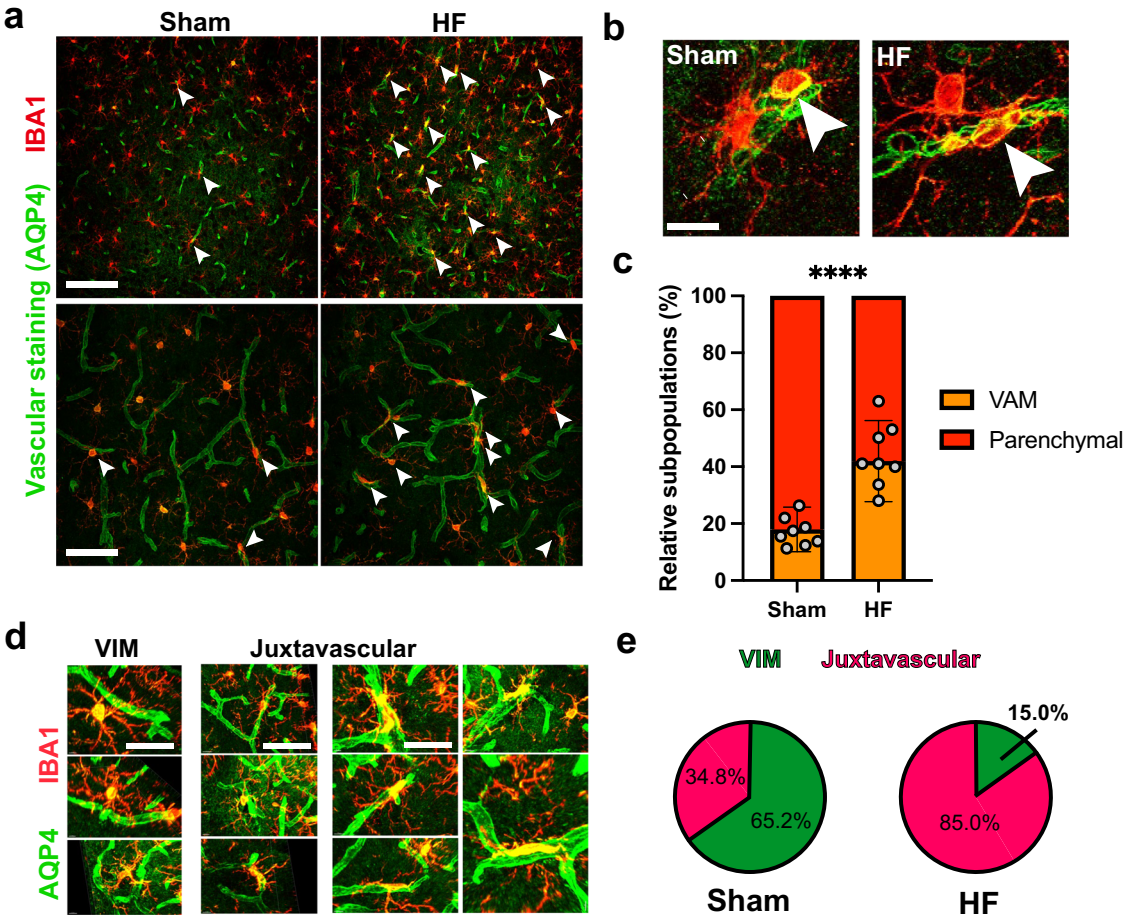

Fig. 1 | Increase in the number of vessel-associated microglia in HF rats. **a** Confocal images show the distribution of parenchymal and vessel-associated microglia in the dorsal hippocampus of sham and HF rats. Immunohistochemical staining against IBA1 (red) and the vessel marker AQP4 (green); white arrowheads indicate vessel-associated microglia. Scale bars 200 µm and 50 µm. **b** High magnification confocal images highlight vessel-associated microglia in sham and HF rats. Scale bar 10 µm. **c** Quantification of vessel-associated microglia in sham and HF rats ($n = 8$ rats per group). ****$p < 0.0001$. **d** Exemplary images (three-dimensional screenshots in Imaris) of Type I–III vessel-associated microglia, which are characterized based on the intensity of microglia-vessel contacts. Type I microglia contact blood vessels exclusively with their filaments, Type II microglia display somatic contact with the blood vessel and Type III seem to merge with the blood vessel along the entirety of the microglial soma. Scale bars, Type I: 25 µm, Type II: 50 µm, and Type II: 25 µm. **e** Pie charts highlight the respective percentage of Type I–III vessel-associated microglia (sham/HF pooled). Error bars throughout the figure represent SEM.

of experiments in which we infused in vivo fluorescently-labeled AngII (intracarotid $AngII_{fluo}$) combined with the fluorescent dye Rhodamine70kDa (Rho70) to label the DH microvasculature, and assessed the location of the leaked $AngII_{fluo}$ in microglial subtypes. Most of the extravasated $AngII_{fluo}$ in the brain parenchyma seemed to accumulate in the extracellular space or on neuronal surfaces as reported before[19,50]. However, some staining was observed to overlap with IBA1-stained microglia. In this case, the vast majority of microglia-bound $AngII_{fluo}$ corresponded to VAM (Fig. 2e–g).

Activation of AT1aRs is a critical signal contributing to the increased abundance of VAM in HF

To determine whether AngII is a signal that contributes to the increased abundance of VAMs in HF, we performed a two-pronged approach. In the first set of experiments, we assessed the effects of an acute increase in circulating AngII levels. To this end, we performed in vivo intracarotid infusions of AngII (or saline as control) combined with the fluorescent dye Rhodamine 70 kDa (Rho70) to label the DH microvasculature, and allowed both substances to circulate for 30 min (Fig. 3a). Processed brain sections of sham and HF rats were then used for immunohistochemical staining to quantify the number of parenchymal microglia and VAM (Fig. 3b). Unexpectedly, we observed that the acute infusion of AngII was sufficient to significantly increase the proportion of VAM in sham rats (1.8-fold). In HF rats, as we reported above, the number of VAM was already significantly higher (2.6-fold) compared to sham rats. Still, AngII further increased the proportion of VAM, albeit to a lesser extent than sham rats (HF: 1.3-fold, Fig. 3c).

TNFα is an important cytokine that stimulates microglia (and other immune cell) recruitment and migration[51–53]. Thus, we combined RNAscope and immunohistochemistry to measure TNFα mRNA expression in microglia cells in sham and HF rats. We found TNFα mRNA to be predominantly expressed in VAMs compared to parenchymal microglia (Fig. S2b), both in Sham (parenchymal: 0.46 ± 0.28 vs 59.24 ± 4.9) and in HF rats (parenchymal: 21.4 ± 4.4 vs 94.08 ± 1.65; mean number of TNFα positive microglial, $n = 4$ rats/group in each sham and HF groups, $p < 0.03$ for both cases, Mann–Whitney test). Given the robust predominance of TNFα in VAMs, subsequent analysis was performed in this subpopulation of microglia cells. (Fig. 3d). We observed that the acute AngII infusion in sham rats increased both the proportion of VAM expressing TNFα (Fig. 3e), as well as the levels of TNFα mRNA within individual VAM (Fig. 3f). In HF rats, we found that virtually all VAM were TNFα mRNA-positive under basal conditions (Fig. 3e), and while relative levels of TNFα mRNA were 2-fold higher in HF rats compared to sham (Fig. 3f), AngII infusion failed to increase expression in this group further.

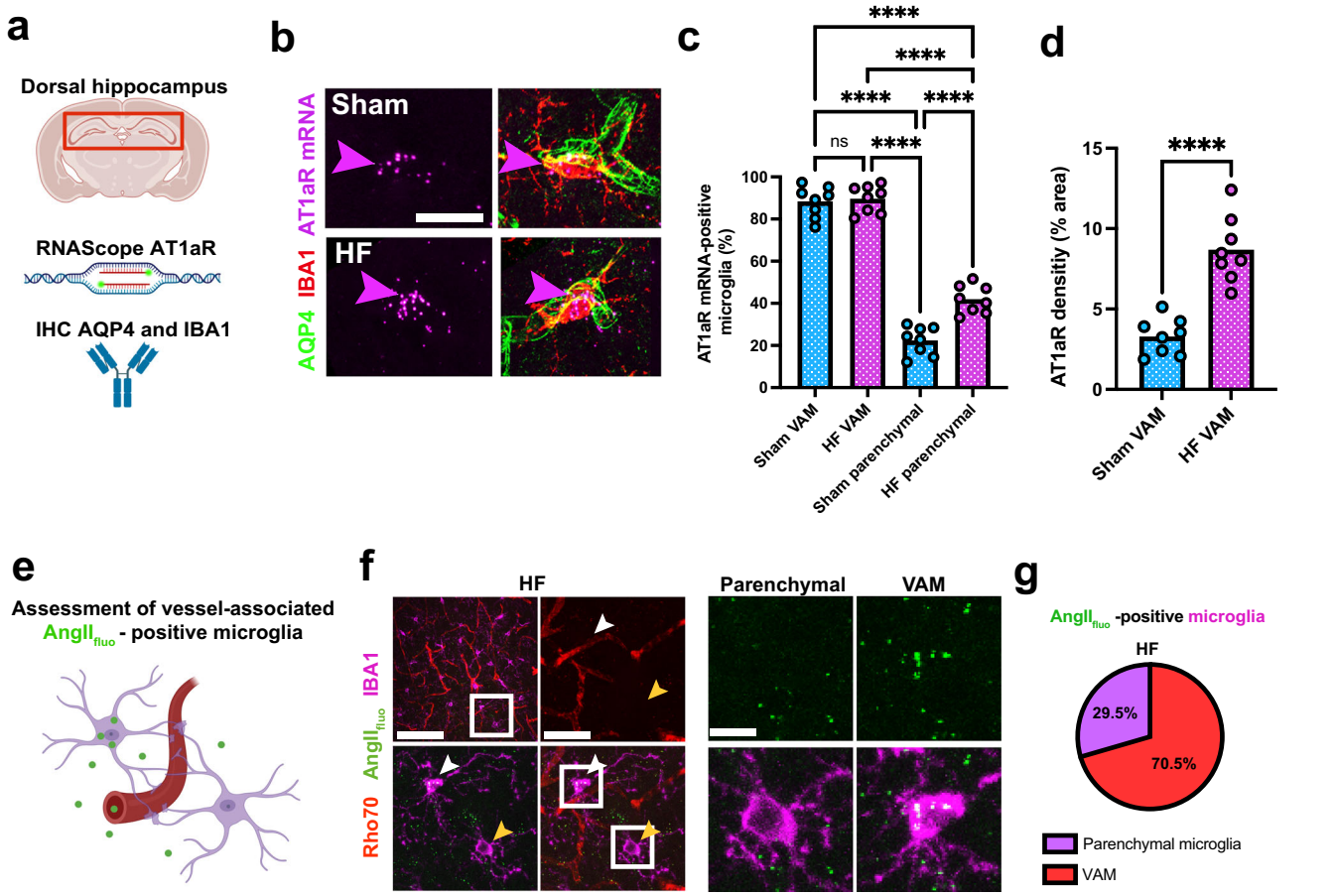

Fig. 2 | Vessel-associated microglia are AT1aR mRNA-positive in both sham and HF rats. a Schematic illustration of the methodological approach to label and identify AT1aR mRNA-positive, vessel-associated microglia in the dorsal hippocampus of sham and HF rats. **b** Confocal images of AT1aR-positive, vessel-associated microglia in sham and HF rats; magenta arrowheads highlight co-localization of IBA1 and AT1aR mRNA. Scale bar 10 µm. **c** Quantification of AT1aR-positive, vessel-associated microglia in sham and HF rats ($n = 8$ rats per group, two-way ANOVA). **d** Assessment of individual AT1aR levels on a cellular level in VAM in sham and HF rats ($n = 8$ rats per group, t-test). **e** Schematic depiction of intracarotid infusions and $AngII_{fluo}$ uptake by microglia. Confocal images of IBA-stained, $AngII_{fluo}$-infused microglia were used for three-dimensional reconstruction and analysis. **f** Confocal images of a typical hippocampus of an HF infused with Rho70 and $AngII_{fluo}$ stained for IBA1. Enlarged insets show a representative example of a VAM and parenchymal microglia, white arrowhead indicates VAM, yellow arrowhead indicates a parenchymal microglia. Enlarged insets (right) show co-localization of $AngII_{fluo}$ in VAM but not parenchymal microglia. Scale bar 100 µm, 25 µm, and 5 µm. **g** Pie charts summarize the percentage of parenchymal and vessel-associated microglia, $AngII_{fluo}$-positive microglia in HF rats.

Finally, and to unequivocally demonstrate that AngII-AT1R signaling is necessary for the increased abundance of VAMs in HF rats, we performed AT1R blockage via administration of losartan, a commonly used AT1R antagonist delivered in the drinking water, as we recently reported[19] (Fig. 4a). The efficacy of the losartan treatment in our hands was verified via measurements of systolic and diastolic blood pressure (Fig. S3). We found that losartan did not affect the proportion of VAM in sham rats (Fig. 4b). Conversely, losartan treatment significantly reduced the proportion of VAM by more than 2-fold in HF rats, normalizing their incidence to levels observed in sham rats (Fig. 4c, d, HF: 45%, HF + Lo: 22%). Moreover, losartan in HF rats also partially normalized to their relative proportions the different types of VAM (i.e., decreased numbers of juxtavascular microglia and a concomitant increase in VIM (chi-square test, $p < 0.0001$, Fig. 4e). Thus, these studies further support a key role for AngII-AT1R signaling in triggering changes in VAM dynamics in the hippocampus of HF rats.

Discussion

In this study, we used a combination of immunohistochemistry, three-dimensional reconstructions of the microglia-vascular interface, in vivo intracarotid infusion of vessel dyes, and fluorescently-labeled AngII, RNAScope hybridization and pharmacological blockade of AngII-AT1aRs to study microglia-vessel dynamics in HF rats. Our main findings are: (i) a 2-fold increase in vessel-associated microglia (VAM) in HF rats; (ii) while AT1aR expression was predominantly confined to VAMs, we observed an increased expression in both VAM and parenchymal microglia in HF rats, (iii) recruitment of microglia to brain capillaries was induced by an acute systemic administration of AngII, and coincided with TNFα upregulation in VAM; and (iv) administration of the AT1aR blocker losartan prevented the recruitment of microglia to brain capillaries, normalizing their levels and subtypes to those found in sham rats. These results underscore and support a highly dynamic microglial-vascular interface in the context of a highly prevalent cardiovascular disease.

Microglia, traditionally considered resident immune cells of the central nervous system, have been recognized for their versatile roles in various pathological conditions beyond the realm of neurological disorders[25,26]. In the context of cardiovascular disease, and particularly HF, a growing body of research has unveiled the significant involvement of microglia in orchestrating neuroinflammatory responses and contributing to the initial stages of the disease[19,24,54,55]. Through the secretion of cytokines, chemokines, and reactive oxygen species, microglia are implicated in the amplification and propagation of neuroinflammatory signals during health and under various disease conditions[25,56–59]. Thus, by influencing synaptic plasticity[60–62], neuronal excitability[63,64], and neurotransmission, microglia mediate neural circuitry modifications that can profoundly affect cardiovascular regulation and homeostasis. Attempting to harness these insights for therapeutic

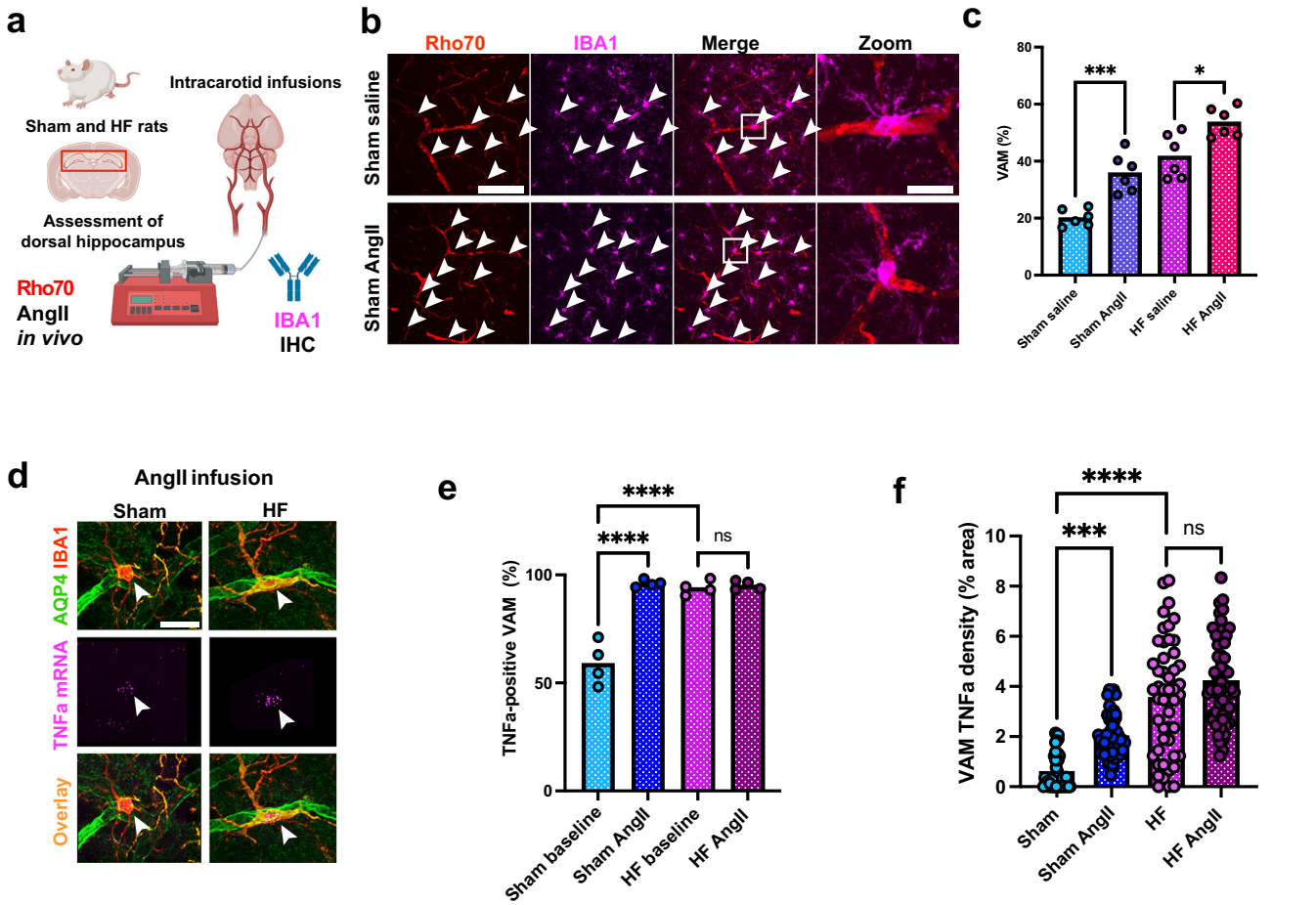

Fig. 3 | AngII-triggered and cytokine-mediated migration of microglia to blood vessels. a Schematic illustration of intracarotid infusions of Rho70 and AngII followed by immunohistochemical staining against IBA1 to label blood vessels and assess the numbers of parenchymal microglia and VAM. **b** Confocal images show parenchymal and VAM in a sham rat infused with saline and a sham rat infused with AngII; white arrowheads indicate the presence of VAM. High magnification shows a VAM in both groups. Scale bars 100 µm and 10 µm. **c** Quantification of vessel-associated microglia after intracarotid AngII infusion ($n = 6$ rats per group, Mann–Whitney). **d** High magnification confocal images showing the co-localization of TNFα mRNA and vessel-associated, IBA1-positive microglia in sham and HF rats at baseline conditions and after intracarotid AngII infusion. White arrowheads highlight TNFα-positive, vessel-associated microglia. Scale bar 10 µm. **e** Quantification of TNFα levels in individual vessel-associated microglia (single cell level area fraction in %) of sham and HF rats at baseline conditions after AngII infusion ($N = 53$ cells from sham rats and $N = 57$ cells from HF rats). **f** Quantification of TNFα-positive, vessel-associated microglia in sham and HF rats ($n = 4$ rats per group) with and without AngII infusions.

benefits, researchers have explored strategies targeting neuroinflammation to ameliorate HF symptoms[19,23,54]. The rat ischemic HF model has been instrumental in evaluating the efficacy of potential interventions[19,24,28,65–67]. Among the proposed interventions, microglia inhibitors have shown promise in attenuating neuroinflammatory responses, potentially dampening the progression of HF[19,66,67].

AngII, a critical player in the pathophysiology of HF, occupies a central position in the cascade of events leading to neurohumoral activation[50,68–72] and cardiac dysfunction[32,73,74]. As HF ensues, AngII levels surge, triggering a cascade of events that heighten sympathetic activity and prompt vascular constriction[32,73–75]. This response is orchestrated to maintain blood pressure in the face of compromised cardiac ejection fraction and to initiate cardiac remodeling[74,75]. Angiotensin receptor blockers such as losartan or angiotensin-converting enzyme (ACE) inhibitors such as captopril are well-established pharmacological approaches for the treatment of patients with HF[76–78], and accumulating evidence supports that they can also act centrally to modulate microglia-mediated neuroinflammation[19,34–36]. Our own previous work highlights the interaction between elevated circulating AngII levels and hippocampal microglial activation, neuronal dysfunction, and apoptosis, and the contribution of this neuroinflammatory cascade to cognitive deficits in the ischemic rat HF model[19]. We further showed that losartan reliably reversed all neuroinflammation-associated endpoints such as microglial morphology, astrogliosis, and increase in cytokine levels, including TNFα, apoptosis, as well as cognitive impairment[19]. Together, these results support a critical role for microglia in mediating AngII-induced neuroinflammation during HF.

The microglia-vascular interface has been the focus of numerous recent studies. Microglia-vascular interactions play a crucial role in maintaining the homeostasis and overall function of the brain[25,26,37,43] and are vital for maintaining the BBB that separates the circulating blood from the brain tissue[37–39,41,79]. Microglia actively survey the brain microenvironment[27,80] and respond to changes in blood vessel integrity[37,43]. In addition, they contribute to immune surveillance, modulate inflammation, and participate in the repair of damaged blood vessels[37]. Importantly, recent work supports their ability to directly regulate local cerebral blood flow[42,43]. Finally, dysregulation of microglia vessel interactions has been implicated in various neurological disorders, including neuroinflammatory and neurodegenerative diseases[38,41]. Still, whether changes in microglia-vascular interactions also occur in the context of cardiovascular diseases, specifically HF, has yet to be determined.

Based on the rationale provided above, we focused on this work on microglial-vascular interactions in the dorsal hippocampus of HF rats.

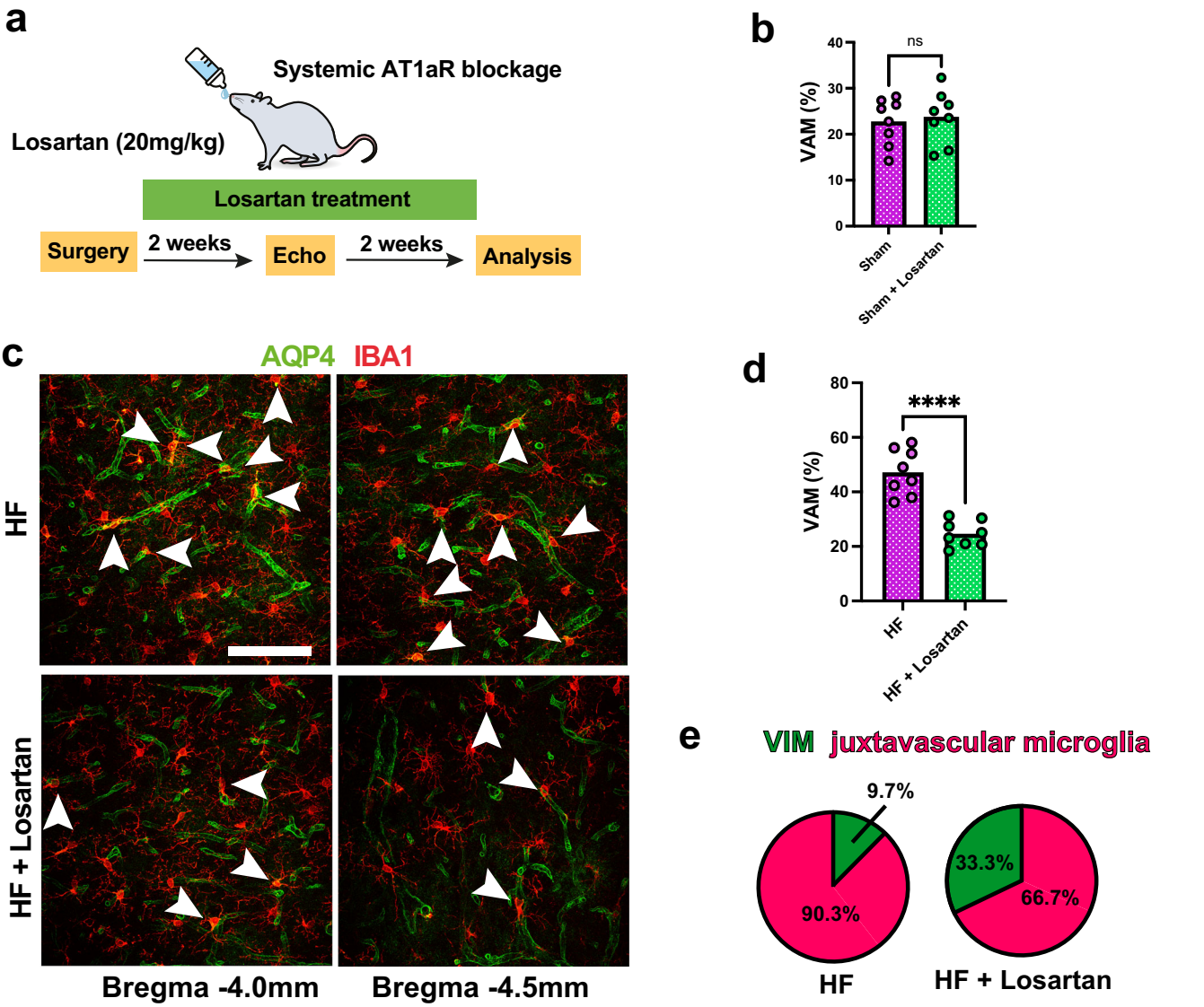

Fig. 4 | Losartan treatment blocks vessel migration in HF but not sham rats. **a** Schematic illustration of losartan administration via drinking water in sham and HF rats. For two weeks after the surgery, losartan (20 mg/kg) was supplied in the drinking water. Following echocardiographic assessment, rats were treated for two more weeks before tissue collection and immunohistochemical staining and analysis. **b** Quantification of the number of vessel-associated and parenchymal microglia after losartan treatment in sham rats ($n = 8$ per group). **c** Confocal images show vessel-associated microglia with and without losartan treatment in HF rats at two different Bregma levels, scale bar 100 µm. **d** Quantification of the number of vessel-associated and parenchymal microglia after losartan treatment in HF rats ($n = 8$ rats per group). **e** Pie charts show the relative percentages of Type I–III vessel-associated microglia with and without losartan treatment in HF rats.

We found that under normal physiological conditions, a small (20–30%) proportion of the hippocampal microglia is directly associated with the local microvasculature (i.e., vascular-associated microglia, VAM), with either processes enwrapping the vascular wall (here defined as vascular interacting microglia, which accounted for the majority of VAMs ~65%, and/or their soma being in direct contact with the vessels (also known as juxta vascular microglia[44,45], which accounted for ~35% of VAMs (Fig. 2). A similar proportion (20%) of VAM was previously reported in other studies[37,43]. In rats with HF, we observed a significant overall increase in the abundance of VAMs (~40%) with a concomitant decrease in parenchymal microglia. These changes were observed using two complementary vascular markers (indirect AQP4 and direct CD31). Moreover, the relative abundance of VAM subtypes reversed in HF rats, juxtavascular being the most predominant (~85%) in this case.

VAMs are in contact with brain capillaries, while perivascular macrophages (PVM) reside on arterioles and venules[44]. Our study shows VAMs predominantly contacting brain capillaries, but we acknowledge the fact that PVM also express IBA1[44] whereby we cannot fully rule out the contribution of this macrophage subpopulation to our pool of VAM. However, based on the fact that the vast majority of analyzed VAM were located on thin brain capillaries and not thicker venules or arterioles, we expect that the contribution of PVM to this pool is insignificant. In addition, we previously reported that the vast majority of IBA1-positive cells are also positive for TMEM119, a marker uniquely expressed in CNS microglia[81].

We report herein that under normal conditions, more than 95% of VAM expressed AT1aR mRNA (Fig. 2). These results suggest that hippocampal VAM could be positioned to sense the elevated levels of circulating AngII that occur during HF[1,19,32,82], thus being a key mechanism initiating a cascade of events leading to upregulation of cytokine expression and release (Fig. 2), further microglial activation[19], further expression of AT1aRs (in both VAMs and parenchymal microglia, Fig. 2), and recruitment of additional microglia to brain capillaries (see model in Fig. 5) in this disease state. This is supported by our study, which showed that an acute elevation of

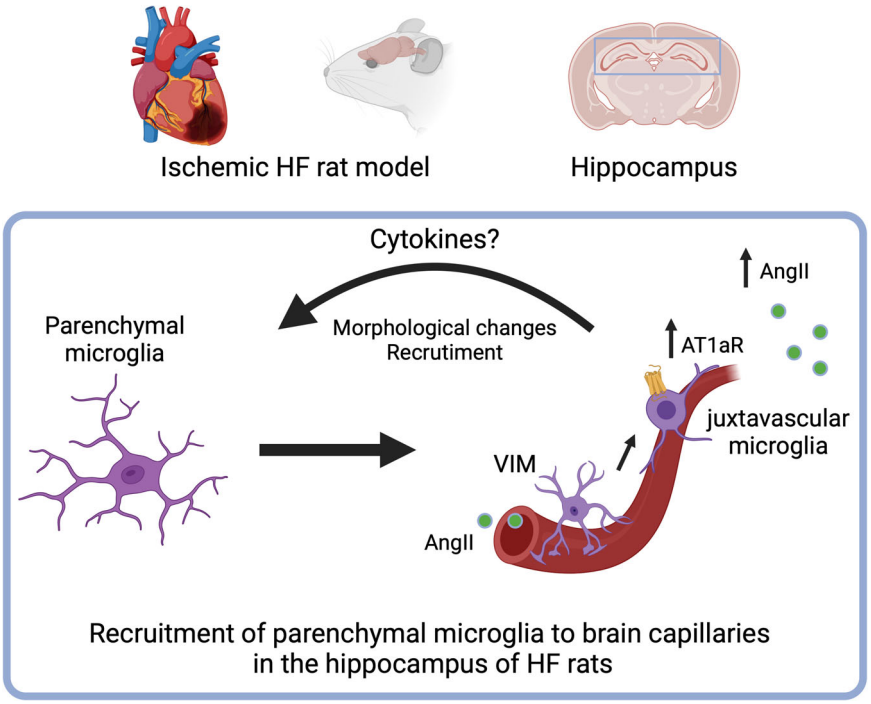

Fig. 5 | Working model for AngII-driven microglial recruitment during heart failure. Based on our current and previous findings, we hypothesize that elevated circulating AngII levels during HF and a subsequent microglia-specific AT1aR upregulation result in increased microglia-vessel interactions due to targeted and local microglial recruitment to brain capillaries. Upon activation, microglia produce and release, among other cytokines, TNFα, which further induces neuroinflammatory signaling, microglial activation, and recruitment to the BBB. This cascade might ultimately result in BBB deterioration and breakdown, allowing leakage of AngII into the hippocampal parenchyma, and further exacerbating neuroinflammation and microglial recruitment to brain capillaries.

circulating levels of AngII was sufficient to increase the number of VAM in sham rats. In HF rats, the number of VAM a was already higher compared to sham rats, but the AngII infusion was still able to further increase the number of VAM in this group. We previously showed that the AngII-AT1aR cascade stimulates the production of several cytokines in hippocampal microglia including C1q, IL1β, and TNFα and that cytokine upregulation correlates with microglial deramification in HF rats[19]. In this study, we focused on TFNα, which was previously shown to be an essential signal that stimulates microglia (and other immune cell) recruitment and migration[51–53]. We found TNFα mRNA, both in sham and HF rats, to be predominantly expressed in VAMs (relative to parenchymal microglia), with a significantly higher number of VAMs expressing TFNα in HF compared to sham rats (Fig. 3). Moreover, TFNα mRNA expression in VAMs was substantially increased in response to an acute infusion of AngII (Fig. 3).

Finally, we found that blocking the actions of endogenous AngII using a clinically relevant AT1R blocker (losartan) following a clinically used route of delivery (oral administration) largely prevented the increase in hippocampal VAM in HF rats. Importantly, we previously reported that this same treatment also prevented the increase in hippocampal TNFα mRNA levels[19]. Of note, we previously did not observe differences in water consumption between rats subjected to losartan treatment and control animals[19]. Together, these results suggest that AngII-AT1aR signaling is critical for dynamic changes in the microglial vascular interface observed during HF.

While our studies support a major role of the AngII-AT1aR signaling cascade in the recruitment and activation of microglia during HF, the precise sequence of events leading to this phenomenon remains to be determined. One possible scenario, as summarized in the working model of Fig. 5, is that the stable population of AT1aR expressing-VAM sense and react to the elevated circulating levels of AngII occurring early in the onset of HF[32,73]. This leads to their overexpression of AT1aRs[83] and the increased production and release of cytokines, including TNFα[84–87], resulting overall in a local neuroinflammatory response at the vascular interface, that ultimately contributes to AngII-mediated disruption of the BBB integrity, as we demonstrated in recent studies[19,24]. Notably, the proportions of $AngII f_{luo}$-positive microglia were similar to that of AT1aR-expressing microglia (Fig. 2c), suggesting that the leaked AngII is binding to those microglia cells expressing AT1aRs. We postulate that the combined action of BBB disruption with concomitant leakage of AngII into the hippocampal parenchyma, along with increased local production and diffusion of cytokines leads to further microglia activation and recruitment to brain capillaries, establishing thus a very disruptive positive feedback loop. Our current working model is in line with our previous study, in which we demonstrated that microglial AngII signaling precedes cytokine production and that administration of losartan in HF rats significantly lowered various cytokine mRNA levels including TNFα[19].

The direct contribution of microglial TNFα to the recruitment and migration of microglial to the vascular interface in HF rats remains undetermined. One possible scenario is that TNFα produced by microglia acts in an autocrine manner[52,88,89]. Alternatively, TNFα could be signaling other local cell types (e.g., astrocytes and endothelial cells) to induce the release of an intermediary signal, yet to be determined. Finally, it is possible that TNFα of a microglial source contributes to the overall pro-inflammatory cascade of events, independent from an action on recruitment and migration.

We acknowledge some important limitations in our studies. Firstly, we did not perform a microglial chemotaxis/migration assay and thus cannot unequivocally prove that AngII signaling is exclusively responsible for HF-induced microglial recruitment to brain capillaries. Secondly, we cannot fully exclude the possibility of artificial, AngII-induced damage of the BBB caused by our intracarotid infusions. However, we believe that this is extremely unlikely for the following reasons: (1) a compromised BBB permeability in HF rats was evident in experiments in which fluo-dextrans were infused[19]; (2) changes in BBB permeability (demonstrated with fluo-dextrans, see ref. 19, were brain-region region specific, arguing against an artificially-induced widespread condition evoked by the i.v. infusion of these compounds; (3) changes in BBB permeability assessed via tight junctions in HF rats were almost completely prevented in Losartan-treated rats[19], supporting that endogenous levels of AngII are sufficient to evoke the changes in BBB reported; In addition, it is important to highlight that the group of Iadecola in a previous work[90], using similar doses/concentrations of ANGII (labeled and not labeled forms, in similar concentrations as those used here, low μM range), demonstrated that an acute AngII infusion failed to induce a change in BBB permeability, which was only observed after slow AngII infusions of at least 14 days.

Collectively, our findings corroborate the key involvement of microglial AngII-AT1aR signaling in the pathophysiology of HF[19], while

providing novel mechanistic insights contributing to this process. Specifically, we provide evidence that AngII-AT1aR signaling leads to rapid, dynamic changes in the microglial-vascular interface, involving the recruitment of microglia cells to the microglial-vascular interface. This remodeling could contribute to critical functional and pathological implications associated with HF, including the disruption of the BBB (as shown here and in our previous study[19]). Moreover, an altered cerebral blood flow and its regulation is typically observed during HF[9,91–93] and is thought to contribute to neuronal damage and cognitive deficits in this condition. Given the growing evidence data supporting a critical role for microglia in regulating cerebral blood flow[42,43], we speculate that the remodeling of the microglial-vascular interface during HF could contribute to dysregulation of cerebral blood flow in this disease. Future studies are clearly needed to determine the functional implications of this remodeling, and to determine whether VAMs, particularly juxtravascular microglial cells themselves have the ability to directly monitor and sense circulating AngII. Notwithstanding, our studies strongly support the notion that the microglial-vascular interface is highly dynamic, and that can be altered in the context of a prevalent cardiovascular disease. Thus, understanding the precise mechanisms and signals involved in this process, as well as their overall impact on BBB disruption, hippocampal neuronal apoptosis, and cognitive deficits during HF[19] is fundamental for the development of novel therapeutic targets for the treatment of cognitive and mood disorders associated with this disease.

Material and methods

All experiments were approved and carried out in agreement with the Georgia State University Institutional Animal Care and Use Committee (IACUC) guidelines. Thus, we have complied with all relevant ethical regulations for animal use.

Animals

We used male Wistar rats (5–7-weeks-old at HF surgery, 180–200 g, Envigo, Indianapolis, IN, USA) for all experiments ($n = 64$). Rats were housed under constant temperature (22 ± 2°C) and humidity (55 ± 5%) on a 12-h light cycle (lights on: 08:00–20:00) ad libitum access to food and water. Our study includes brain tissue from animals that have been used for another study previously[19]. These tissues were used for data presented in Figs. 1 and 4.

Heart failure surgery and echocardiography

To induce HF in rats, coronary artery ligation surgery was performed. To induce anesthesia, animals were placed in a chamber containing 5% isoflurane mixed with O_2 (100% O_2, 1 L/min). Optimum anesthesia was checked by the absence of limb withdrawal reflex to a painful stimulus (hind paw pinch). Then animals were intubated for mechanical ventilation until the end of the surgical procedure. During the whole procedure, anesthesia was adequately maintained using 2-3% isoflurane delivered by a vaporizer machine mixed with O_2 (100% O_2, 1 L/min). Maintenance of anesthesia was checked periodically by the absence of limb withdrawal reflex. Heart failure survival surgery was performed maintaining an aseptic surgical technique. Fur from the left chest area was clipped and underlying skin was disinfected with 70% ethanol followed by 5% povidone-iodine. A perpendicular (to midline) skin incision was made from the midline to the left mid-axillary line. Pectoral muscles were dissected by blunt dissection. Hemostasis was achieved by electro-cauterization (Geiger Medical technologies-150A, USA). A small incision was made in the third intercostal space and a retractor was applied to retract the 3rd and 4th ribs. The thymus was lifted upwards with forceps and the pericardium was removed with a second pair of forceps. To ensure consistency in the position of the left anterior descending (LAD) coronary artery occlusion, the apex of the left atrium and the conus of the right ventricle were used as landmarks for inserting and extracting the needle. The heart was exteriorized and a 'Prolene 6-0' suture (Ethicone, USA) was inserted just beneath the left atrial base along the interventricular septum to make a loop around the main diagonal branch of the LAD coronary artery. Finally, myocardial infarction was induced by ligating the LAD coronary artery. Since 2/3rd of the left ventricular blood supply is provided by the LAD coronary artery, occlusion of the LAD coronary artery results in a pale discoloration of the left ventricle, which guides as a visual confirmation of the ischemic left ventricle following LAD coronary artery ligation. Four to five weeks after the surgery we performed transthoracic echocardiography (Vevo 3100 systems; Visual Sonics, Toronto, ON; Canada) under light isoflurane (2–3%) anesthesia. The ejection fraction (EF) obtained via echocardiography was used as a key parameter to determine the degree of functional HF[10,24,94]. The mean EF values for sham and HF rats were 82.27 ± 3.2 and 25.22 ± 6.29, respectively ($p < 0.0001$).

Immunohistochemistry

Following pentobarbital-induced anesthesia (Euthasol, Virbac, ANADA #200-071, Fort Worth, TX, USA, Pentobarbital, 80 mg/kgbw, i.p.), rats were first perfused at a speed of 20 mL/min with 0.01 M PBS (200 mL, 4 °C) through the left ventricle followed by 4% paraformaldehyde (PFA, in 0.3 M PBS, 200 mL, 4 °C), while the right atrium was opened with an incision. Brains were post-fixed for 24 h in 4% PFA at 4 °C and transferred into a 30% sucrose solution (in 0.01 M PBS) at 4 °C for 3–4 days. For immunohistochemistry, 40 µm slices were cut using a Leica Cryostat (CM3050 S), and brain slices were kept in 0.01 M PBS at 4 °C until used for staining. Brain slices were blocked with 5% Normal Horse Serum in 0.01 M PBS for 1 h at room temperature. After a 15-min washing in 0.01 M PBS, brain slices were incubated for 24 h in 0.01 M PBS, 0.1% Triton-X, 0.04% NaN_3 containing different antibodies: 1:1000 of anti-IBA1 (polyclonal rabbit, Wako, 019-19741, Lot: CAK1997) or 1:500 of anti-AQP-4 (polyclonal rabbit, Alomone labs, AQP-004) at room temperature. Following 15-min washing in 0.01 M PBS, sections were incubated in 0.01 M PBS, 0.1% Triton-X, 0.04% NaN_3 with 1:500 Alexa Fluor 488/594-conjugated donkey anti-rabbit (Jackson ImmunoResearch, 711-585-152 and 705-585-147) for 4 h at RT. Double immunohistochemical staining against AQP4 and IBA1 (both polyclonal rabbits) was performed in two individual rounds with washing 3 × 10 min in PBS and subsequent blocking to minimize potential cross-reactivity of the primary and secondary antibodies. For the triple staining following antibodies and concentrations were used: M/R CD31 AF3621 from R&D Systems at 1:333, AQP4 249–323 from Alomone Labs at 1:333, and IBA1 234–308 from Synaptic Systems at 1:500. Brain slices were washed again for 15 min in 0.01 M PBS and mounted using antifade mounting medium (Vectashield with DAPI, H-1200B/H-1500). Euthanasia was induced by an overdose of sodium pentobarbital (80 mg/kgbw i.p.).

RNAScope in situ hybridization

RNAScope reagents were bought from acdbio (PN320881). Nuclease-free water and PBS were acquired from Fisher Scientific. Brain tissues were handled according to the procedure outlined for Immunohistochemistry, utilizing nuclease-free PBS, water, PBS, and sucrose, in accordance with the instructions provided by the manufacturer. To evaluate the data, microglia were categorized as mRNA-positive if they exhibited three or more fluorescently labeled voxel units within their individual cell bodies. Probes targeting AT1aR or TNFα mRNA (both C1, rat) were purchased from acdbio. Euthanasia was induced by an overdose of sodium pentobarbital (80 mg/kgbw i.p.).

Confocal microscopy and 3D analysis of microglia via Imaris

Confocal images were obtained using a Zeiss LSM 780 confocal microscope (1024 × 1024 pixel, 16-bit depth, pixel size 0.63-micron, zoom 0.7). Three-dimensional reconstruction of microglia was performed using Imaris software[24]. For the analysis of VAM microglia, the surface-to-surface and surface-to-volume ratio feature of Imaris was used after prior enabling of object-to-objects statistics. To avoid potential cross-reactivity of AQP4 and IBA1 signals that might confound subsequent data analysis, any AQP4-positive voxels within microglia were removed through the creation of a new masked channel. Thus, only 'vessel-specific' AQP4 signal outside of microglia was used for the analysis of microglia-vessel interaction. Microglia were defined as juxta vascular microglia if they had overlapping surfaces

with blood vessels of > 2 μm² to avoid sampling of false positives as a result of reconstruction artifacts. VIM (microglia in close proximity to blood vessels) microglia displayed filamentous contacts, without somatic contact (i.e., distance from soma to vessel > 1 μm); juxta vascular microglia displayed somatic contact with vessels (i.e., distance from soma to vessel < 1 μm) or displayed somatic contact with vessels (i.e., distance from soma to vessel < 1 μm) and extensive soma-vessel overlap defined as total surface-to-surface ratio > of > 8 μm². Whether the microglia had multiple vessel contacts was not taken into account for the final analysis. For reasons of simplicity, VIM and juxtavascular microglia are referred to as VAM in some of the Figures.

Assessment of microglial $AngII_{fluo}$ uptake

Rats were anesthetized using a mixture of Ketamine and Xylazine (at concentrations of 60 mg/mL and 8 mg/mL, respectively). A non-occluding catheter was inserted into the left internal carotid artery. Subsequently, $AngII_{fluo}$ (at a concentration of 3 μmol/L, obtained from Anaspec, CA) was infused at a rate of 2.86 μL/g/rat and allowed to circulate for a duration of 30 min[50]. After this period, the rats were decapitated, and their brains were fixed and sliced into sections that were 40 μm thick using a Cryostat. These sections were prepared for confocal imaging. The software Imaris was utilized to identify and quantify the presence of microglial $AngII_{fluo}$ using object-to-object statistics and quantification of engulfed $AngII_{fluo}$ volume (in μm³). Microglia were considered to be $AngII_{fluo}$ when they contained >2 μm³ $AngII_{fluo}$ to avoid sampling of false positives as a result of reconstruction artifacts.

Losartan treatment

Rats with heart failure (HF) were assigned randomly to either the HF group or the HF + Losartan group. Losartan at a dose of 20 mg/kg/day was administered in the drinking water, commencing one week after the HF surgery and continuing until the rats were sacrificed for analysis four to six weeks after the surgery.

Statistical analyses

Statistical analyses were carried out using GraphPad Prism 9 (GraphPad Software, California, USA). To compare groups, various tests were employed, including Student's *t*-test, chi-square test, and one- or two-way analysis of variance (ANOVA), followed by Tukey post-hoc tests. For group size and power calculations, we used the following assumptions: effect size: 1.5, significance 0.05, and power 0.70. The incidence of effects was compared using chi-square tests. Data was checked for normality prior to statistical analysis via parametric tests. In cases of low sample sizes, the Mann–Whitney test was used as indicated. The results are denoted as mean ± standard error of the mean (SEM). Statistical significance was established at $p < 0.05$. In the corresponding figures, significance levels were indicated as $^{*}p < 0.05$, $^{**}p < 0.01$, and $^{***}p < 0.0001$.

Reporting summary

Further information on research design is available in the Nature Portfolio Reporting Summary linked to this article.

Data availability

The data supporting this study's findings were included as Supplementary data.

Received: 22 December 2023; Accepted: 7 November 2024;
Published online: 19 November 2024

References

1. Metra, M. & Teerlink, J. R. Heart failure. *Lancet* **390**, 1981–1995 (2017).
2. Groenewegen, A., Rutten, F. H., Mosterd, A. & Hoes, A. W. Epidemiology of heart failure. *Eur. J. Heart Fail* **22**, 1342–1356 (2020).
3. Bui, A. L., Horwich, T. B. & Fonarow, G. C. Epidemiology and risk profile of heart failure. *Nat. Rev. Cardiol.* **8**, 30–41 (2011).
4. Dunlay, S. M., Weston, S. A., Jacobsen, S. J. & Roger, V. L. Risk factors for heart failure: a population-based case-control study. *Am. J. Med.* **122**, 1023–1028 (2009).
5. Khatibzadeh, S., Farzadfar, F., Oliver, J., Ezzati, M. & Moran, A. Worldwide risk factors for heart failure: a systematic review and pooled analysis. *Int. J. Cardiol.* **168**, 1186–1194 (2013).
6. Mueller, K. et al. Brain damage with heart failure: cardiac biomarker alterations and gray matter decline. *Circ. Res.* **126**, 750–764 (2020).
7. Hammond, C. A. et al. Long-term cognitive decline after newly diagnosed heart failure: longitudinal analysis in the CHS (cardiovascular health study). *Circ. Heart Fail* **11**, e004476 (2018).
8. Hay, M. et al. Cognitive impairment in heart failure: a protective role for angiotensin-(1-7). *Behav. Neurosci.* **131**, 99–114 (2017).
9. Zuccala, G. et al. Left ventricular dysfunction: a clue to cognitive impairment in older patients with heart failure. *J. Neurol. Neurosurg. Psychiatry* **63**, 509–512 (1997).
10. Parent, M. B. et al. Heart failure impairs mood and memory in male rats and down-regulates the expression of numerous genes important for synaptic plasticity in related brain regions. *Behav. Brain Res*. https://doi.org/10.1016/j.bbr.2021.113452 (2021).
11. Toledo, C. et al. Cognitive impairment in heart failure is associated with altered Wnt signaling in the hippocampus. *Aging* **11**, 5924–5942 (2019).
12. Woo, M. A. et al. Regional hippocampal damage in heart failure. *Eur. J. Heart Fail* **17**, 494–500 (2015).
13. Suzuki, H. et al. Structural abnormality of the hippocampus associated with depressive symptoms in heart failure rats. *Neuroimage* **105**, 84–92 (2015).
14. Bird, C. M. & Burgess, N. The hippocampus and memory: insights from spatial processing. *Nat. Rev. Neurosci.* **9**, 182–194 (2008).
15. Palmer, J. A. et al. Hippocampal blood flow rapidly and preferentially increases after a bout of moderate-intensity exercise in older adults with poor cerebrovascular health. *Cereb. Cortex* **33**, 5297–5306 (2023).
16. Steventon, J. J. et al. Hippocampal blood flow is increased after 20 min of moderate-intensity exercise. *Cereb. Cortex* **30**, 525–533 (2020).
17. Colasanti, A. et al. Hippocampal neuroinflammation, functional connectivity, and depressive symptoms in multiple sclerosis. *Biol. Psychiatr.* **80**, 62–72 (2016).
18. Ho, Y. H. et al. Peripheral inflammation increases seizure susceptibility via the induction of neuroinflammation and oxidative stress in the hippocampus. *J. Biomed. Sci.* **22**, 46 (2015).
19. Althammer, F. et al. Angiotensin II-mediated neuroinflammation in the hippocampus contributes to neuronal deficits and cognitive impairment in heart failure rats. *Hypertension* https://doi.org/10.1161/HYPERTENSIONAHA.123.21070 (2023).
20. Mowry, F. E., Peaden, S. C., Stern, J. E. & Biancardi, V. C. TLR4 and AT1R mediate blood–brain barrier disruption, neuroinflammation, and autonomic dysfunction in spontaneously hypertensive rats. *Pharmacol. Res*. https://doi.org/10.1016/j.phrs.2021.105877 (2021).
21. Moreira, J. D. et al. Inhibition of microglial activation in rats attenuates paraventricular nucleus inflammation in Galphai2 protein-dependent, salt-sensitive hypertension. *Exp. Physiol.* **104**, 1892–1910 (2019).
22. Wu, K. L., Chan, S. H. & Chan, J. Y. Neuroinflammation and oxidative stress in rostral ventrolateral medulla contribute to neurogenic hypertension induced by systemic inflammation. *J. Neuroinflammation* **9**, 212 (2012).
23. Diaz, H. S., Toledo, C., Andrade, D. C., Marcus, N. J. & Rio, R. D. Neuroinflammation in heart failure: NEW insights for an old disease. *J. Physiol.* https://doi.org/10.1113/JP278864 (2019).
24. Althammer, F. et al. Three-dimensional morphometric analysis reveals time-dependent structural changes in microglia and astrocytes in the central amygdala and hypothalamic paraventricular nucleus of heart failure rats. *J. Neuroinflammation* **17**, 221 (2020).

25. Prinz, M., Jung, S. & Priller, J. Microglia biology: one century of evolving concepts. *Cell* **179**, 292–311 (2019).
26. Prinz, M. & Priller, J. Microglia and brain macrophages in the molecular age: from origin to neuropsychiatric disease. *Nat. Rev. Neurosci.* **15**, 300–312 (2014).
27. Nimmerjahn, A., Kirchhoff, F. & Helmchen, F. Resting microglial cells are highly dynamic surveillants of brain parenchyma in vivo. *Science* **308**, 1314–1318 (2005).
28. Patel, V. B., Zhong, J. C., Grant, M. B. & Oudit, G. Y. Role of the ACE2/angiotensin 1–7 axis of the renin-angiotensin system in heart failure. *Circ. Res* **118**, 1313–1326 (2016).
29. Wang, K., Basu, R., Poglitsch, M., Bakal, J. A. & Oudit, G. Y. Elevated angiotensin 1-7/angiotensin II ratio predicts favorable outcomes in patients with heart failure. *Circ. Heart Fail* **13**, e006939 (2020).
30. Schunkert, H. et al. Regulation of intrarenal and circulating renin-angiotensin systems in severe heart failure in the rat. *Cardiovasc Res.* **27**, 731–735 (1993).
31. van de Wal, R. M. et al. Determinants of increased angiotensin II levels in severe chronic heart failure patients despite ACE inhibition. *Int J. Cardiol.* **106**, 367–372 (2006).
32. Opie, L. H. & Sack, M. N. Enhanced angiotensin II activity in heart failure: reevaluation of the counterregulatory hypothesis of receptor subtypes. *Circ. Res.* **88**, 654–658 (2001).
33. Shao, Q. et al. Modification of sarcolemmal Na+-K+-ATPase and Na+/Ca2+ exchanger expression in heart failure by blockade of renin-angiotensin system. *Am. J. Physiol. Heart Circ. Physiol.* **288**, H2637–H2646 (2005).
34. Park, H. S. et al. Chronically infused angiotensin II induces depressive-like behavior via microglia activation. *Sci. Rep.* **10**, 22082 (2020).
35. Sun, H. et al. Angiotensin II and its receptor in activated microglia enhanced neuronal loss and cognitive impairment following pilocarpine-induced status epilepticus. *Mol. Cell Neurosci.* **65**, 58–67 (2015).
36. Benicky, J. et al. Angiotensin II AT1 receptor blockade ameliorates brain inflammation. *Neuropsychopharmacology* **36**, 857–870 (2011).
37. Haruwaka, K. et al. Dual microglia effects on blood brain barrier permeability induced by systemic inflammation. *Nat. Commun.* **10**, 5816 (2019).
38. Zhao, Z., Nelson, A. R., Betsholtz, C. & Zlokovic, B. V. Establishment and dysfunction of the blood–brain barrier. *Cell* **163**, 1064–1078 (2015).
39. Rubin, L. L. & Staddon, J. M. The cell biology of the blood–brain barrier. *Annu Rev. Neurosci.* **22**, 11–28 (1999).
40. Risau, W. & Wolburg, H. Development of the blood–brain barrier. *Trends Neurosci.* **13**, 174–178 (1990).
41. Thurgur, H. & Pinteaux, E. Microglia in the neurovascular unit: blood–brain barrier-microglia interactions after central nervous system disorders. *Neuroscience* **405**, 55–67 (2019).
42. Csaszar, E. et al. Microglia modulate blood flow, neurovascular coupling, and hypoperfusion via purinergic actions. *J. Exp. Med.* https://doi.org/10.1084/jem.20211071 (2022).
43. Bisht, K. et al. Capillary-associated microglia regulate vascular structure and function through PANX1-P2RY12 coupling in mice. *Nat. Commun.* **12**, 5289 (2021).
44. Mondo, E. et al. A developmental analysis of juxtavascular microglia dynamics and interactions with the vasculature. *J. Neurosci.* **40**, 6503–6521 (2020).
45. Grossmann, R. et al. Juxtavascular microglia migrate along brain microvessels following activation during early postnatal development. *Glia* **37**, 229–240 (2002).
46. Lassmann, H., Zimprich, F., Vass, K. & Hickey, W. F. Microglial cells are a component of the perivascular glia limitans. *J. Neurosci. Res.* **28**, 236–243 (1991).
47. Hablitz, L. M. et al. Circadian control of brain glymphatic and lymphatic fluid flow. *Nat. Commun.* **11**, 4411 (2020).
48. Alvarez-Vergara, M. I. et al. Non-productive angiogenesis disassembles Ass plaque-associated blood vessels. *Nat. Commun.* **12**, 3098 (2021).
49. Gehrmann, J., Matsumoto, Y. & Kreutzberg, G. W. Microglia: intrinsic immuneffector cell of the brain. *Brain Res. Brain Res. Rev.* **20**, 269–287 (1995).
50. Biancardi, V. C., Son, S. J., Ahmadi, S., Filosa, J. A. & Stern, J. E. Circulating angiotensin II gains access to the hypothalamus and brain stem during hypertension via breakdown of the blood–brain barrier. *Hypertension* **63**, 572–579 (2014).
51. Liddelow, S. A. et al. Neurotoxic reactive astrocytes are induced by activated microglia. *Nature* **541**, 481–487 (2017).
52. Bras, J. P. et al. TNF-alpha-induced microglia activation requires miR-342: impact on NF-kB signaling and neurotoxicity. *Cell Death Dis.* **11**, 415 (2020).
53. D'Mello, C., Le, T. & Swain, M. G. Cerebral microglia recruit monocytes into the brain in response to tumor necrosis factoralpha signaling during peripheral organ inflammation. *J. Neurosci.* **29**, 2089–2102 (2009).
54. Wang, H. W. et al. Inhibition of inflammation by minocycline improves heart failure and depression-like behaviour in rats after myocardial infarction. *PLoS One* **14**, e0217437 (2019).
55. Rana, I. et al. Microglia activation in the hypothalamic PVN following myocardial infarction. *Brain Res.* **1326**, 96–104 (2010).
56. Olah, M. et al. Single cell RNA sequencing of human microglia uncovers a subset associated with Alzheimer's disease. *Nat. Commun.* **11**, 6129 (2020).
57. Masuda, T. et al. Spatial and temporal heterogeneity of mouse and human microglia at single-cell resolution. *Nature* **566**, 388–392 (2019).
58. Wendeln, A. C. et al. Innate immune memory in the brain shapes neurological disease hallmarks. *Nature* **556**, 332–338 (2018).
59. Erny, D. et al. Host microbiota constantly control maturation and function of microglia in the CNS. *Nat. Neurosci.* **18**, 965–977 (2015).
60. Lehrman, E. K. et al. CD47 protects synapses from excess microglia-mediated pruning during development. *Neuron* **100**, 120–134 e126 (2018).
61. Schafer, D. P. et al. Microglia sculpt postnatal neural circuits in an activity and complement-dependent manner. *Neuron* **74**, 691–705 (2012).
62. Paolicelli, R. C. et al. Synaptic pruning by microglia is necessary for normal brain development. *Science* **333**, 1456–1458 (2011).
63. Cserep, C. et al. Microglia monitor and protect neuronal function through specialized somatic purinergic junctions. *Science* **367**, 528–537 (2020).
64. Badimon, A. et al. Negative feedback control of neuronal activity by microglia. *Nature* **586**, 417–423 (2020).
65. Patel, K. P. Role of paraventricular nucleus in mediating sympathetic outflow in heart failure. *Heart Fail Rev.* **5**, 73–86 (2000).
66. Guggilam, A. et al. Cytokine blockade attenuates sympathoexcitation in heart failure: cross-talk between nNOS, AT-1R and cytokines in the hypothalamic paraventricular nucleus. *Eur. J. Heart Fail* **10**, 625–634 (2008).
67. Prickaerts, J., Raaijmakers, W. & Blokland, A. Effects of myocardial infarction and captopril therapy on anxiety-related behaviors in the rat. *Physiol. Behav.* **60**, 43–50 (1996).
68. Pitra, S., Worker, C. J., Feng, Y. & Stern, J. E. Exacerbated effects of prorenin on hypothalamic magnocellular neuronal activity and vasopressin plasma levels during salt-sensitive hypertension. *Am. J. Physiol. Heart Circ. Physiol.* **317**, H496–H504 (2019).
69. Yu, Y., Wei, S. G., Weiss, R. M. & Felder, R. B. Angiotensin II type 1a receptors in the subfornical organ modulate neuroinflammation in the hypothalamic paraventricular nucleus in heart failure rats. *Neuroscience* **381**, 46–58 (2018).

70. Biancardi, V. C., Stranahan, A. M., Krause, E. G., de Kloet, A. D. & Stern, J. E. Cross talk between AT1 receptors and Toll-like receptor 4 in microglia contributes to angiotensin II-derived ROS production in the hypothalamic paraventricular nucleus. *Am. J. Physiol. Heart Circ. Physiol.* **310**, H404–H415 (2016).
71. Stern, J. E. et al. Astrocytes contribute to angiotensin II stimulation of hypothalamic neuronal activity and sympathetic outflow. *Hypertension* **68**, 1483–1493 (2016).
72. Kang, Y. M. et al. Cross-talk between cytokines and renin-angiotensin in hypothalamic paraventricular nucleus in heart failure: role of nuclear factor-kappaB. *Cardiovasc Res.* **79**, 671–678 (2008).
73. Zablocki, D. & Sadoshima, J. Angiotensin II and oxidative stress in the failing heart. *Antioxid. Redox Signal* **19**, 1095–1109 (2013).
74. De Mello, W. C. & Danser, A. H. Angiotensin II and the heart : on the intracrine renin-angiotensin system. *Hypertension* **35**, 1183–1188 (2000).
75. Unger, T. & Li, J. The role of the renin-angiotensin-aldosterone system in heart failure. *J. Renin Angiotensin Aldosterone Syst.* **5**, S7–S10 (2004).
76. Pitt, B. et al. Effect of losartan compared with captopril on mortality in patients with symptomatic heart failure: randomised trial-the Losartan heart failure survival study ELITE II. *Lancet* **355**, 1582–1587 (2000).
77. Pitt, B. et al. Randomised trial of losartan versus captopril in patients over 65 with heart failure (Evaluation of Losartan in the Elderly Study, ELITE). *Lancet* **349**, 747–752 (1997).
78. Crozier, I. et al. Losartan in heart failure. Hemodynamic effects and tolerability. Losartan hemodynamic study group. *Circulation* **91**, 691–697 (1995).
79. Matcovitch-Natan, O. et al. Microglia development follows a stepwise program to regulate brain homeostasis. *Science* **353**, aad8670 (2016).
80. Tremblay, M. E. et al. The role of microglia in the healthy brain. *J. Neurosci.* **31**, 16064–16069 (2011).
81. Bennett, M. L. et al. New tools for studying microglia in the mouse and human CNS. *Proc. Natl. Acad. Sci. USA* **113**, E1738–E1746 (2016).
82. Cohn, J. N. Sympathetic nervous system in heart failure. *Circulation* **106**, 2417–2418 (2002).
83. Wei, S. G., Yu, Y., Zhang, Z. H. & Felder, R. B. Angiotensin II upregulates hypothalamic AT1 receptor expression in rats via the mitogen-activated protein kinase pathway. *Am. J. Physiol. Heart Circ. Physiol.* **296**, H1425–H1433 (2009).
84. Abadir, P. M., Walston, J. D., Carey, R. M. & Siragy, H. M. Angiotensin II Type-2 receptors modulate inflammation through signal transducer and activator of transcription proteins 3 phosphorylation and TNFalpha production. *J. Interferon Cytokine Res.* **31**, 471–474 (2011).
85. Garcia Fragas, M. & Gastao Davanzo, G. Cross-talk between TNF-alpha and Angiotensin II in the Neural Control of Hypertension. *J. Neurosci.* **41**, 7512–7513 (2021).
86. Rosa, A. C., Rattazzi, L., Miglio, G., Collino, M. & Fantozzi, R. Angiotensin II induces tumor necrosis factor-alpha expression and release from cultured human podocytes. *Inflamm. Res.* **61**, 311–317 (2012).
87. Ruiz-Ortega, M. et al. Angiotensin II regulates the synthesis of proinflammatory cytokines and chemokines in the kidney. *Kidney Int. Suppl.* https://doi.org/10.1046/j.1523-1755.62.s82.4.x (2002).
88. Block, M. L., Zecca, L. & Hong, J. S. Microglia-mediated neurotoxicity: uncovering the molecular mechanisms. *Nat. Rev. Neurosci.* **8**, 57–69 (2007).
89. Kuno, R. et al. Autocrine activation of microglia by tumor necrosis factor-alpha. *J. Neuroimmunol.* **162**, 89–96 (2005).
90. Faraco, G. et al. Perivascular macrophages mediate the neurovascular and cognitive dysfunction associated with hypertension. *J. Clin. Invest* **126**, 4674–4689 (2016).
91. Alves, T. C. & Busatto, G. F. Regional cerebral blood flow reductions, heart failure and Alzheimer's disease. *Neurol. Res.* **28**, 579–587 (2006).
92. Gruhn, N. et al. Cerebral blood flow in patients with chronic heart failure before and after heart transplantation. *Stroke* **32**, 2530–2533 (2001).
93. Qiu, C. et al. Heart failure and risk of dementia and Alzheimer disease: a population-based cohort study. *Arch. Intern Med.* **166**, 1003–1008 (2006).
94. Biancardi, V. C. et al. Contribution of central nervous system endothelial nitric oxide synthase to neurohumoral activation in heart failure rats. *Hypertension* **58**, 454–463 (2011).

Acknowledgements

Schematic illustrations of Figs. 2, 3, 4, and 5 have been created using biorender.com. J.E.S. received funding from NINDS 094640 and HL162575-01. R.K.R. received funding from the American Heart Association grant 916907. M.K.K. received funding from NIH K99HL168434 and F.A. received funding from the DFG Emmy Noether starting grant AL 2466/2-1.

Author contributions

F.A. acquisition, analysis, or interpretation of data for the work, conception, or design of the work. R.K.R.: acquisition, analysis, or interpretation of data for the work. M.K.K.: acquisition, analysis, or interpretation of data for the work. Y.P.: acquisition, analysis, or interpretation of data for the work. J.H.: acquisition, analysis, or interpretation of data for the work. S.M.: acquisition, analysis, or interpretation of data for the work. E.C.L.: acquisition, analysis, or interpretation of data for the work. J.E.S.: conception or design of the work and acquisition of funding.

Competing interests

The authors declare no competing interests.

Additional information

Supplementary information The online version contains supplementary material available at https://doi.org/10.1038/s42003-024-07229-8.

Correspondence and requests for materials should be addressed to Javier E. Stern.

Peer review information *Communications Biology* thanks Sebastien Foulquier and the other, anonymous, reviewer(s) for their contribution to the peer review of this work. Primary Handling Editor: Dario Ummarino.